Journal of Physics: Condensed Matter

PAPER

Recovery of photoexcited magnetic ordering in Sr_2IrO_4

To cite this article: Jiemin Li *et al* 2019 *J. Phys.: Condens. Matter* **31** 255801

IOP Publishing Journal of Physics: Condensed Matter
J. Phys.: Condens. Matter **31** (2019) 255801 (5pp) https://doi.org/10.1088/1361-648X/ab123d

Recovery of photoexcited magnetic ordering in Sr_2IrO_4

Jiemin Li[1,2], Ruitang Wang[1,2], Haizhong Guo[3], Yi Zhu[4], Yue Cao[5,6], Jian Liu[7], Hong Ding[1,2], Haidan Wen[4] and X Liu[8]

[1] Beijing National Laboratory for Condensed Matter Physics and Institute of Physics, Chinese Academy of Sciences, Beijing 100190, People's Republic of China
[2] School of Physics, University of Chinese Academy of Sciences, Beijing 100049, People's Republic of China
[3] School of Physical Engineering, Zhengzhou University, Zhengzhou 450001, People's Republic of China
[4] Advanced Photon Source, Argonne National Laboratory, Argonne, IL 60439, United States of America
[5] Condensed Matter Physics and Material Science Department, Brookhaven National Laboratory, Upton, NY 11973, United States of America
[6] Materials Science Division, Argonne National Laboratory, 9700 Cass Ave, Lemont, IL 60439, United States of America
[7] Department of Physics and Astronomy, University of Tennessee, Knoxville, TN 37996, United States of America
[8] School of Physical Science and Technology, ShanghaiTech University, Shanghai 201210, People's Republic of China

E-mail: liuxr@shanghaitech.edu.cn

Received 30 January 2019, revised 8 March 2019
Accepted for publication 21 March 2019
Published 9 April 2019

Abstract

The recovery of antiferromagnetic and lattice order of Sr_2IrO_4 upon laser excitation was measured by time-resolved x-ray diffraction on nanosecond time scales. The *in situ* measurements of both magnetic and lattice order parameters allow direct comparison of their time evolutions without ambiguity. We found that the magnetic order recovers with two time constants. The fast sub-nanosecond recovery is associated with the re-establishment of three dimensional antiferromagnetic order while the slow sub-nanosecond recovery agrees with the lattice cooling on tens of nanoseconds. The strong oscillating behavior of magnetic order during the long time recovery may be related to complicated dynamics of defect-pinned magnetic domains.

Keywords: pump-probe, resonant x-ray scattering, long-time scale, magnetism, iridates

(Some figures may appear in colour only in the online journal)

1. Introduction

Recent advances in synchrotron techniques and the quick development of x-ray free-electron-laser facilities open opportunities to track the long-range orders of transient non-equilibrium states in strongly correlated materials in real time [1–3]. With laser excitation, charge, spin, orbital and lattice in these systems can be heavily disturbed, resulting in a wide variety of ultrafast behaviours, such as the transition between metal and insulator in manganites [4–6], the emergence of short-lived superconductivity in cuprates [7] or K_3C_{60} [8] and the transient melting of long-range magnetic/orbital order in $La_{1/2}Sr_{3/2}MnO_4$ [9, 10], etc. However, the relaxation processes following the initial ultrafast evolution are less explored. Beaurepaire *et al* [11] proposed a model using three linked heat reservoirs where the charge, spin and lattice subsystems evolve with different temperatures but are coupled with mutual interactions. As the charge recovery happens at a very short time scale, examining the long time recovery of charge, spin and lattice could serve as a new approach to study their couplings. For example, the unexpected decoupling of charge and lattice degrees of freedom had been found to slow down on a time scale of hundreds of nanoseconds (ns) in the long-range ordered $La_{1/3}Sr_{2/3}FeO_3$ [12]. However, the spin-lattice coupling

on a comparable time scale in correlated systems has not been directly measured. The responses of magnetic [13] and lattice [14] to laser perturbation in Sr_2IrO_4 were only reported separately, but how these two order parameters couple during the recovery is not clear because of the different experimental conditions, techniques, and samples used in previous experiments.

In this work, we had employed time-resolved x-ray resonant elastic magnetic scattering (REMS) to investigate the recovery of antiferromagnetic ordering as well as the lattice relaxation of Sr_2IrO_4 with a time resolution of 0.1 ns and up to tens of ns. As a spin-orbital coupling (SOC) induced Mott insulator, Sr_2IrO_4 has been extensively studied in recent years [15–19]. The SOC splits the t_{2g} manifold of the Ir 5*d* states into the so called $j_{\text{eff}} = \frac{3}{2}$ and $j_{\text{eff}} = \frac{1}{2}$ states (see figure 1(a)), with the latter half occupied. Owing to the large spatial extension, the 5*d* orbitals, where the spins reside, are expected to experience a significant magnetoelastic coupling in Sr_2IrO_4 [20–22], hence making it a good platform to explore the dynamics of spin-lattice coupling. The high energy photons at Ir L_3-edge (∼11.215 keV) cover a sizeable range in the reciprocal space so that both of structural and magnetic Bragg peaks can be tracked. During the experiments, the evolution of the structure recovery was monitored under the same experimental condition as the magnetic ordering. We found that the structure peak recovers exponentially, with a recovery time constant of 6.6 ns. The magnetic peak initially recovers in an exponential fashion with a time constant of 0.4 ns, consistent with our earlier report [13]. However, this fast process is absent in lattice recovery, a clear indication of decoupling of spin and lattice in sub nanosecond time scale. Beyond 2 ns, the magnetic ordering enters a slow recovery similar to that of the lattice. In this long recovery time region, we find the measured magnetic recovery becomes semi-oscillatory, with a fluctuating amplitude larger than the noise level. We suggest that this is due to non-uniform formation of magnetic domains associated with various types of defects after the laser pumping, i.e. different magnetically ordered domains in the probing volume may possess different recovery time scales and the domain size may also experience growth and shrinkage, highlighting a possible mesoscopic effect that is not included in the simple three-thermal-reservoir model [11].

2. Experiments

Sr_2IrO_4 thin films with ∼80 unit-cells (∼200 nm) were grown on $SrTiO_3$ substrates by pulsed laser deposition [23]. Pump and probe REMS measurements were carried out at the advanced photon sources at beamline 7-ID-C with a horizontal diffraction geometry (see figure 1(b)). The laser pulse with a central wavelength of 1240 nm and pulse duration of ∼100 fs was obtained from an optical parametric amplifier pumped by a Ti:Sa laser system at 1 kHz repetition rate and impinged on the sample surface at an angle of 47°. The x-ray pulse with a pulse duration of 100 ps was tuned to Ir L_3-edge (11.215 keV) and came to sample surface at 5° to maximize the overlap of illuminating volume with laser pulse. The evolution of the magnetic ordering as a function of recovery time was monitored with resonant x-ray scattering intensity of the (1 0 16) magnetic ordering Bragg peak [17]. The resonant scattering condition of (1 0 16) at the Ir L_3-edge was pre-determined from energy dependent fluorescence scans. For comparison, the (0 0 16) structural peak was also measured. All data were collected with Pilatus detector at $T \sim 70$ K, well below the Neel ordering temperature of 240 K [24]. To avoid possible extrinsic effects, the laser fluence on sample was kept as low as 1.8 mJ cm^{-2}. The time resolution was determined as 0.1 ns, limited by the temporal width of x-ray pulse from a synchrotron facility.

3. Data and results

After optimizing all scattering angles for (1 0 16) magnetic ordering peak, the integrated scattering intensity on the detector was monitored to study its time evolution. The optical conductivity spectra revealed the energy scales for the transitions between the $j_{\text{eff}} = \frac{1}{2}$ and $j_{\text{eff}} = \frac{3}{2}$ states in Sr_2IrO_4 [25]. With a 1240 nm (1 eV) laser pumping to excite electrons mainly from the $j_{\text{eff}} = \frac{3}{2}$ to $j_{\text{eff}} = \frac{1}{2}$ states (see the inset in figure 1(b)), a hole is created in the $j_{\text{eff}} = \frac{3}{2}$ manifold, and locally $j_{\text{eff}} = \frac{1}{2}$ state becomes doubly occupied. Such pumped intermediate electronic configuration strongly perturbs the long range magnetic ordering. The resulted suppression of the magnetic ordering is clearly captured in our experiment as shown in figure 2, where (a), (c) and (b), (d) compare the scattering intensity of the magnetic peak at 1 ns before (negative time) and 0.2 ns after (positive time) the laser pumping respectively. Obviously, the scattering intensity significantly decreases at +0.2 ns, although it is not completely quenched due to the partial recovery of magnetic order at 0.2 ns [13] and the mismatch between the pump (∼100 nm) [26] and the probe depth (200 nm, the film thickness). The suppression and recovery of the magnetic scattering intensity was monitored up to +15 ns.

As the excited electron recombines with the hole in the $j_{\text{eff}} = \frac{3}{2}$ band, concurrent with the recovery of antiferromagnetic correlation, the absorbed energy is transferred into the lattice degree of freedom, leading to thermal expansion. This is evident from the Bragg peak shift in figure 3, where we overlay the rocking scans of the (0 0 16) structure peak before and after the laser pumping. The red curve shows their difference, which is largest at the rising and falling edges instead of the peak position. Since the peak shift is small, the diffraction intensity of the structural peak at the half-rising edges is proportional to the change of the lattice constant. As a result, we are able to monitor the lattice recovery as a result of the film cooling by recording the diffraction intensity as a function of time at a fixed rocking angle (vertical dashed line).

With the monitored signals in our experiments explained above, the measured evolution of the lattice and the magnetic ordering upon laser pumping is summarized in figure 4, in which we plot the time response of the intensities for both (0 0 16) and (1 0 16). The data was fitted with exponential recovery functions. For the lattice recovery, the measured (0 0 16) Bragg peak intensity can be well fitted by

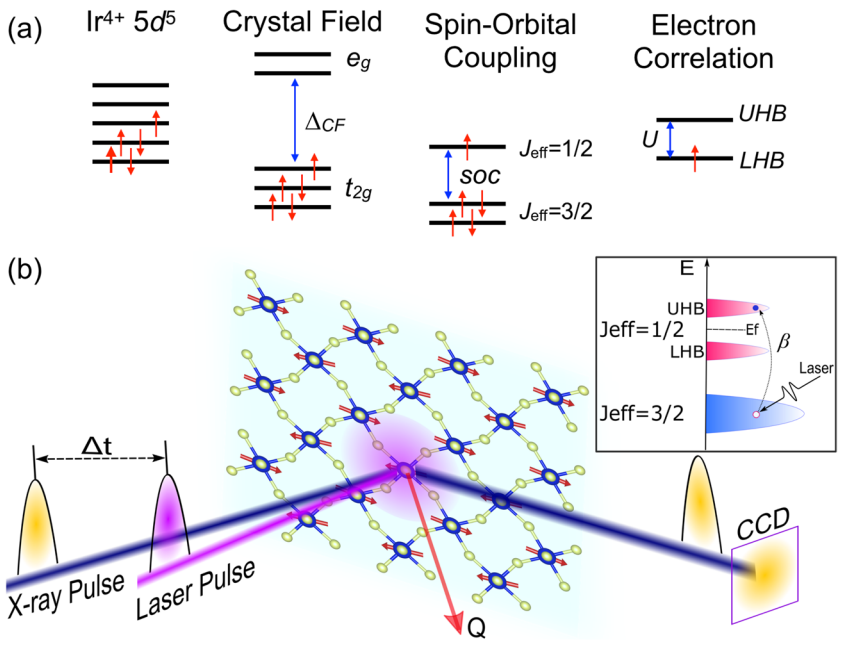

Figure 1. (a) Energy splitting of $5d^5$ electronic configuration in Sr_2IrO_4. The octahedral crystal field (Δ_{CF}) and strong SOC interaction work together to introduce the full-filled $j_{eff} = \frac{3}{2}$ quartet, and the half-filled $j_{eff} = \frac{1}{2}$ doublet which hosts moderate on-site Coulomb repulsion. (b) Experimental setup. The pumping laser (shown in purple) excites electrons from $j_{eff} = \frac{3}{2}$ to the half occupied $j_{eff} = \frac{1}{2}$ states as illustrated in the inset, followed by the x-ray pulse (shown in yellow) at 11.215 keV to monitor the Bragg peak intensities at a delayed time.

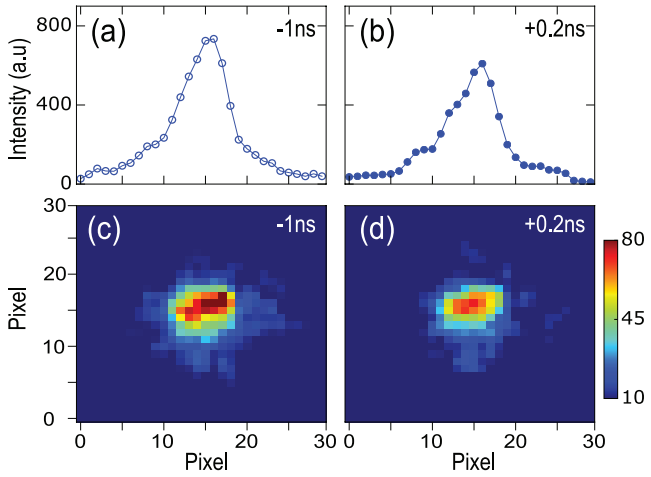

Figure 2. Intensity variation of the (1 0 16) magnetic Bragg peak at 1 ns before ((a), (c)) and 0.2 ns after ((b), (d)) the 1.8 mJ cm^{-2} laser pump. (a) and (b) are from the vertical integration of image (c) and (d) respectively.

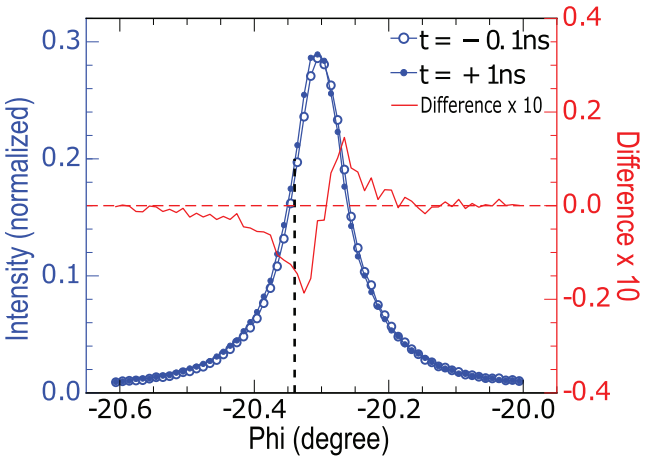

Figure 3. The sample phi angle rocking scan across the (0 0 16) structural peak at 0.1 ns before (blue balls) and 1 ns after (blue dots) the laser pumping pulses. The red curve shows their difference, which is scaled by a factor of ten for clarity. Vertical dashed black line shows the off-set phi angle chosen for time dependent measurements.

function $I = A_1 e^{-t/\tau_1} + B$ with a single recovery time constant $\tau_1 = 6.6$ ns, consistent with previous reports [14]. Up to ~25 ns, the structure is fully recovered. In striking contrast to the simple behavior of structure response, the magnetic ordering behaves in a more complicated way. In the first 2 ns, it shows a quick exponential recovery. Beyond ~2 ns, the recovery becomes slower and is heavily dressed by other effects, appearing as the oscillation of measured peak intensities which is larger than the noise level. To account for the two time scales, the magnetic signal was fitted with bi-exponential function $I = A_2 e^{-t/\tau_2} + A_3 e^{-t/\tau_3} + C$. The strong oscillation beyond 2 ns prevents a reliable fitting to the slow exponential. Thus τ_3 was constrained to be the same as τ_1 from the lattice recovery, and all other parameters are freely fitted. The solid blue line in figure 4 shows the overall agreement between our fitting and the experimental data. The extracted fast recovery constant τ_2 for the spin recovery is 0.4 ns, compatible with the earlier studies [13, 26].

4. Discussion

Our experimental results reveal two time scales for magnetic ordering of Sr_2IrO_4 during a time range from 0.1 to 15 ns. The shorter recovery below 2 ns was well fitted with a

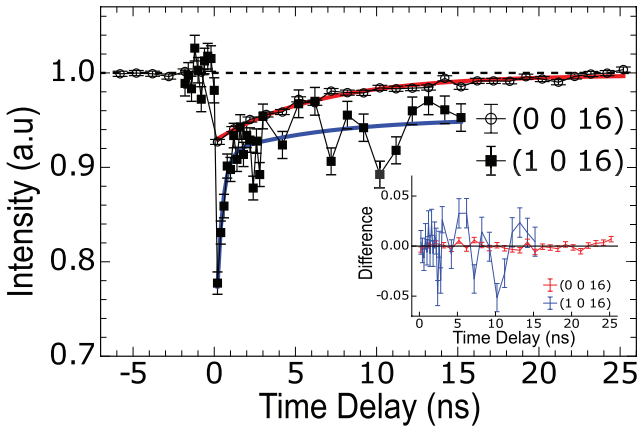

Figure 4. Structural and magnetic peak intensity evolution as a function of probe delay time. Black empty ball is for the (0 0 16) peak and black filled square is for the (1 0 16) peak. The error bars show shot noise. Red and blue lines are the fitting results. The inset displays the differences between the fitting and experimental results for the magnetic (blue) and structural (red) respectively.

time constant of 0.4 ns, an order-of-magnitude smaller than the lattice recovery time scale of 6.6 ns, which suggests that the initial recovery is unrelated to the lattice, but an intrinsic dynamics of the spin degree of freedom itself. In our previous reports [13], this recovery was postulated to be the re-establishment of the inter-plane three dimensional magnetic ordering. The comparison to the lattice recovery in this report provides direct experimental evidence to show the decoupling of the spin and lattice order on this time scale.

As for the longer time scale, the recovery of the magnetic peak (1 0 16) to ∼15 ns seems to follow the lattice cooling, indicating a strong spin-lattice coupling as argued by the magnetic and thermal measurements [20]. However, the oscillation in experimental data can not be well modeled by a simple exponential behavior [11], as demonstrated by the remarkable deviation from exponential fitting over a longer time scale in the inset of figure 4. The nature of strong oscillatory behavior may suggest the complex recovery pathway that involves the competition of domain growth and shrinking close to phase transition [27]. Because all the data points were from measurements averaging tens of thousands of laser pulses, any random domain formation and fluctuation should be well averaged. Likely, the nucleation of local domains associated with different sample defects behaves differently, and their thermal activated fusion into each other takes even longer time. Such hypothesis is supported by the observation that the noise of the signal at negative time is undoubtedly weaker, indicating the large oscillating behaviour is likely an intrinsic response of the antiferromagnetic order. As the experiment was carried out with 1 kHz laser pulse train with 1 millisecond (ms) interval, the negative timing can be viewed as x-ray pulse coming in ∼1 ms after the laser pumping. Obviously, such mesoscopic process is not covered in the simplified exponential recovery consideration.

5. Conclusion

We have used synchrotron-based pump-probing technique to study the recovery of the magnetic ordering and its coupling with the lattice in Sr_2IrO_4. The magnetic ordering shows two recovery time scales. The initial sub nanosecond time scale recovery is decoupled from the lattice cooling while the longer time recovery of the magnetic Bragg peak is consistent with the lattice cooling, indicating the spin-lattice energy exchange is sufficient to reach the same temperature on the time scale of ns. In addition, the recovery curve beyond 2 ns is surprisingly oscillatory, possibly due to mesoscopic competitions among magnetic domains.

Acknowledgments

Work at ShanghaiTech University was partially supported by MOST of China under the Grant No.2016YFA0401000. JML and RTW was supported by international partnership program of Chinese Academy of Scinces under the Grant No.112111KYSB20170059. HZG was supported by the National Natural Science Foundation of China (Grant No. 11574365). YC acknowledges support from both Brookhaven National Laboratory and Argonne National Laboratory. Brookhaven National Laboratory was supported by the U.S. Department of Energy, Office of Basic Energy Sciences, Division of Materials Sciences and Engineering, under Contract No. DE-SC0012704. Argonne National Laboratory was supported by the U.S. Department of Energy, Office of Basic Energy Sciences, under Contract No. DE-AC0206CH11357. JL acknowledges the support of the Science Alliance Joint Directed Research & Development Program and the Organized Research Unit Program at the University of Tennessee. HW acknowledge the support of U.S. Department of Energy (DOE), Office of Science and Basic Energy Sciences (BES), Materials Sciences and Engineering Division. The use of the Advanced Photon Source is supported by DOE-BES, under Contract No. DE-AC02-06CH11357. HD is supported by grants from the Ministry of Science and Technology of China (2016YFA0401000, 2015CB921300) and the Chinese Academy of Sciences (XDB07000000).

ORCID iDs

Jiemin Li https://orcid.org/0000-0002-7153-6123

References

[1] Aoki H, Tsuji N, Eckstein M, Kollar M, Oka T and Werner P 2014 *Rev. Mod. Phys.* **86** 779–837
[2] Zhang J and Averitt R D 2014 *Annu. Rev. Mater. Res.* **44** 19–43
[3] Thielemann-Kohn N, Schick D, Pontius N, Trabant C, Mitzner R, Holldack K, Zabel H, Fohlisch A and Scher-Langeheine C 2017 *Phys. Rev. Lett.* **119** 197202
[4] Kiryukhin V, Casa D, Hill J P, Keimer B, Vigliante A, Tomioka Y and Tokura Y 1997 *Nature* **386** 813–5
[5] Miyano K, Tanaka T, Tomioka Y and Tokura Y 1997 *Phys. Rev. Lett.* **78** 4257
[6] Takubo N, Onishi I, Takubo K, Mizokawa T and Miyano K 2008 *Phys. Rev. Lett.* **101** 177403

[7] Fausti D, Tobey R I, Dean N, Kaiser S, Dienst A, Hoffmann M C, Pyon S, Takayama T, Takagi H and Cavalleri A 2011 *Science* **331** 189–91
[8] Mitrano M *et al* 2016 *Nature* **530** 461–4
[9] Tobey R I, Prabhakaran D, Boothroyd A T and Cavalleri A 2008 *Phys. Rev. Lett.* **101** 197404
[10] Ehrke H *et al* 2011 *Phys. Rev. Lett.* **106** 217401
[11] Beaurepaire E, Merle J C, Daunois A and Bigot J Y 1996 *Phys. Rev. Lett.* **76** 4250
[12] Zhu Y, Hoffman J, Rowland C, Park H, Walko D, Freeland J, Ryan P, Schaller P, Bhattacharya A and Wen H 2018 *Nat. Commun.* **9** 1799
[13] Dean M *et al* 2016 *Nat. Mater.* **12** 601–5
[14] Li Y, Richard D S, Zhu M, Walko D A, Kim J, Ke X, Miao L and Mao Z Q 2016 *Sci. Rep.* **6** 19302
[15] Cosio-Castaneda C, Tavizon G, Baeza A, de la Mora P and Escudero R 2007 *J. Phys.: Condens. Matter.* **19** 446210
[16] Kim B J *et al* 2008 *Phys. Rev. Lett.* **101** 076402
[17] Kim B J, Ohsumi H, Komesu T, Sakai S, Morita T, Takagi H and Arima T 2009 *Science* **323** 1329–32
[18] Jackeli G and Khaliullin G 2009 *Phys. Rev. Lett.* **102** 017205
[19] Kim Y K, Krupin O, Denlinger J D, Bostwick A, Rotenberg E, Zhao Q, Mitchell J F, Allen J W and Kim B J 2014 *Science* **345** 187–90
[20] Chikara S, Korneta O, Crummett W P, DeLong L W, Schlottmann P and Cao G 2009 *Phys. Rev.* B **80** 140407
[21] Torchinsky D H, Chu H, Zhao L, Perkins N B, Sizyuk Y, Qi T, Cao G and Hsieh D 2015 *Phys. Rev. Lett.* **114** 096404
[22] Ye F, Chi S, Chakoumakos B C, Fernandez-Baca J A, Qi T and Cao G 2013 *Phys. Rev.* B **87** 140406
[23] Rayan-Serrao C *et al* 2013 *Phys. Rev.* B **87** 085121
[24] Crawford M K, Subramanian M A, Harlow R L, Fernandez-Baca J A, Wang Z R and Johnston D C 1994 *Phys. Rev.* B **49** 9198
[25] Moon S J, Jin H, Choi W S, Lee J S, Seo S S A, Yu J, Cao G, Noh T W and Lee Y S 2009 *Phys. Rev.* B **80** 195110
[26] Krupin O *et al* 2016 *J. Phys.: Condens. Matter* **28** P32LT01
[27] Porter D A and Easterling K E 2009 *Phase Transformations in Metals and Alloys* (Boca Raton, FL: CRC Press)